Stroboscopic Imaging to Determine Number Density of Acoustic Cavitation Bubbles

ストロボ撮影による音響キャビテーション気泡数密度の計測

Takanobu Kuroyama[1†] ([1]NIT, Gifu College)
黒山 喬允 [1†] ([1]岐阜高専)

1. Introduction

Acoustic cavitation is a phenomenon in which many microbubbles are generated in water by intense ultrasound. The bubbles oscillate due to pressure changes caused by the ultrasound, and at the time of maximum contraction, the inside of the bubble becomes hot and pressurized, causing various mechanical and chemical effects[1)]. The effects of the bubble greatly depends on the bubble characteristics, such as the size distribution and number density, and it is necessary to measure these characteristics to estimate the effects of the bubbles[2, 3)].

Microscopic imaging of the bubbles directory provides morphological information of the bubbles, but as the number density of the bubbles increases, it becomes difficult to recognize the bubble shape due to the bubbule occlusion. In addition, since the depth of field of the microscopy system is unknown, it is difficult to obtain the number density of bubbles from a single image.

In this paper, to reduce the contrast loss of bubble images due to bubble occlusion, a shallow depth of field imaging system is employed to acquire bubble image. The depth of field of the imaging system is revealed by analyzing the images while scanning in the direction of the optical axis and the spatial distribution of the number density of the bubbles under the ultrasonic horn is revealed.

2. Measurement principle

Figure 1 shows the experimental system of the proposed method. An ultrasonic transducer with a horn is immerged into the water in a glass vessel. The ultrasound from the horn surface generates acoustic cavitation bubbles. The frequency of the ultrasound is 19.4 kHz and the diameter of the output surface of the horn is 30 mm. The generated bubbles distribute near the output surface of the horn and form the cone-like bubble structure (CBS).

The bubbles are radiated from divergent light from a Xe flash lamp with a duration of 240 ns. Shadowgraph images of the bubble are captured by an image sensor with a lens system. The light axis of the lens system and that of the Xe flash lamp are not aligned with each other to reduce the depth of field. The imaging system consists of lenses and an image sensor is scanned by a z-stage. The image sensor acquires the image of bubbles distributed 1.5 mm below the center of the horn.

Figure 2(a) shows a shadowgraph image of the bubbles obtained with the measurement system. The radius of the bubbles and minimum brightness of the image in the bubble region is automatically detected with image recognition as shown in Fig. 2(b). The minimum brightness in the bubble region depends on the z-displacement of the bubble from the plane of the focus of the lens system. We assume that the minimum brightness of the bubble image only depends on the distance from the plane of the focus and the radius of the bubble.

The imaging system is scanned along the z-axis with interval δz. The z-position of the plane of focus is $\delta z l$ where l is a natural number. The number of bubbles, whose diameter is a and minimum brightness ${}^aC$ is between ${}^aC_k$ and ${}^aC_{k+1}$, ${}^aN_k^l$, is counted by the image recognition. Let z-displacement of the bubble from the plane of focus be z_d and let the minimum brightness ${}^aC$ of the bubble located at $z_{k+1} > |z_\mathrm{d}| \geq z_k$ satisfies ${}^aC_{k+1} > {}^aC \geq {}^aC_k$. Here, we assume that ${}^aC$ does not depend on

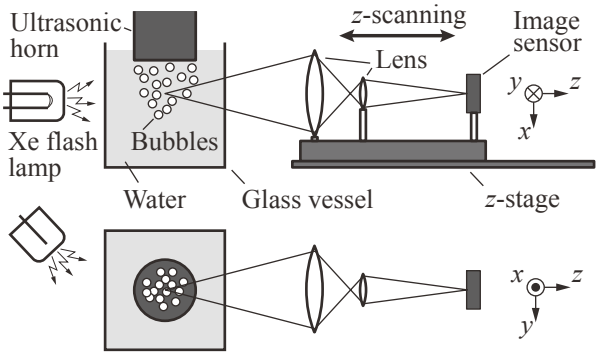

Fig. 1 Experimental setup.

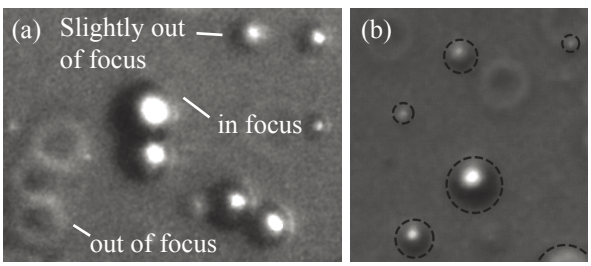

Fig. 2 Measurement principle of proposed method (a) an example of bubble image. (b) Result of automatic image recognition. Dashed lines show the detected perimeter of the bubbles.

† kuroyama@gifu-nct.ac.jp

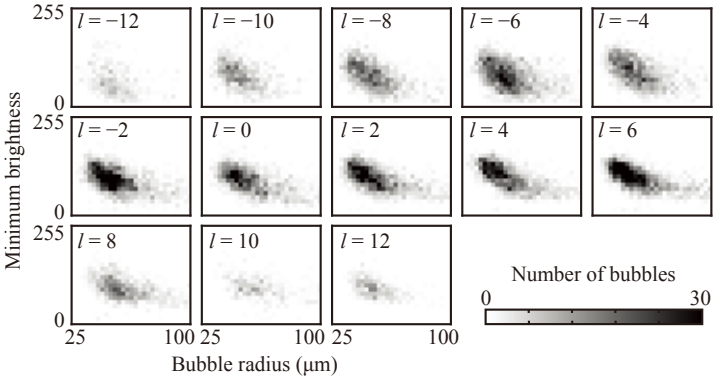

Fig. 3 Distribution of bubble radius and minimum brightness. The natural number l from −12 to 12 corresponds to displacement of imaging system from −6 mm to 6mm.

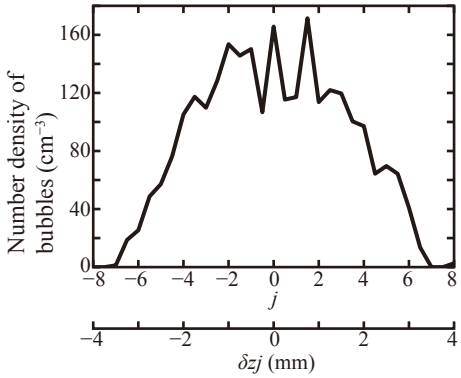

Fig. 4 Number density distribution of bubbles with radius between 45 μm to 65 μm.

the sign of the z_d, namely the z dependence of C is assumed to be symmetric with the plane of focus. Then, when $z_{k+1} - z_k = \delta z$, the flowing equations hold.

$$\mathbf{A}\,{}^a\boldsymbol{\nu} = {}^a\mathbf{N}, \quad (1)$$

$${}^a\mathbf{N} = [{}^aN_0{}^{-L} \cdots {}^aN_k{}^{-L} \cdots {}^aN_M{}^{-L} \ \cdots {}^aN_k{}^{l} \cdots {}^aN_M{}^{L}]^{\mathrm{T}}, \quad (2)$$

$$\mathbf{A} = [A_{ij}], \quad (3)$$

$${}^a\boldsymbol{\nu} = S\delta z\,{}^a\boldsymbol{\rho}, \quad (4)$$

$${}^a\boldsymbol{\rho} = [{}^a\rho_{-L} \ \cdots \ {}^a\rho_0 \ \cdots \ {}^a\rho_l \ \cdots \ {}^a\rho_L]^{\mathrm{T}}. \quad (5)$$

where S, ${}^a\boldsymbol{\rho}$, and ${}^a\boldsymbol{\nu}$ are the area of image, the number density of the bubble, and the number of bubbles within the volume of $S\delta z$, respectively. The element of $\mathbf{A}$ in row i and column j, A_{ij}, is expressed as

$$A_{ij} = \begin{cases} 1 & (i = (M+1)(l+L) + k + 1, \\ & \quad j = (l+L) \pm k + 1) \\ 0 & (\text{otherwise}) \end{cases} \quad (6)$$

where $(2L+1)(M+1) \geq i > 0$ and $2L+1 \geq j > 0$. Solving Eq. 1 for ${}^a\boldsymbol{\nu}$ based on the vector ${}^a\mathbf{N}$ obtained with the experiment, the spatial distribution of the bubble number density in the z-direction, ${}^a\boldsymbol{\rho}$, can be obtained. Since ${}^a\boldsymbol{\nu}$ is the number of bubbles and a positive number, the non-negative least squares method is used to obtain the solution. The intervals of the minimum brightness

$${}^a\mathbf{C} = [C_0{}^a \ \cdots \ C_k{}^a \ \ C_M{}^a]$$

is unknown. Thus, based on the results of the calculation of ${}^a\boldsymbol{\nu}$, we also perform a nonlinear optimization for ${}^a\mathbf{C}$ to minimize the following residual

$$\| {}^a\mathbf{N} - \mathbf{A}\,{}^a\boldsymbol{\rho} \|,$$

where $\| \ \|$ means the Euclidean norm.

3. Experimental results and discussion

Figure 3 shows the relationship between the minimum brightness of the image and the bubble radius determined by the computational image analysis. In this figure, the total number of bubbles detected from 100 images is shown in the shade of gray. The z-scanning of the imaging system was performed with 0.5 mm intervals, but the results at several representative points are shown in the figure. The displacement δzj of 0 corresponds to the position of the ultrasonic horn axis. The minimum brightness decreases as the bubble radius increases because the contrast transfer characteristics of the optical system decayed at high spatial frequencies. Bubbles with a radius of 30 μm or less are not detected due to the resolution and contrast transfer characteristics of the imaging system. As approaching $\delta zj = 0$, the number density of the larger bubbles increases, and the minimum brightness decreases. This implies that the bubbles with large diameter mainly distribute around the horn axis.

Figure 4 shows the number density distribution of bubbles with a radius between 45 μm to 65 μm. To calculate the bubble density, we used the sum of the number of bubbles for 100 images at each δzj. Therefore, the bubble density in Fig. 4 is a time-averaged value. The number of bubbles detected in each image varies, and in some images, the number of bubbles was up to three times the average number. Thus, it is considered that the density of the number of bubbles can be several times higher than the value in Fig. 4 at some moments.

4. Conclusion

The number density of bubbles was estimated from the bubble images by an analysis considering the depth of field of the imaging system. It was found that the number density of bubbles under the horn exceeded 100 cm^{-3} but these values are for bubbles with a radius of 45 to 65 um and do not take into account the variability caused by bubble oscillation. We will discuss these points in detail in the future.

Acknowledgment

This work was supported by JSPS KAKENHI Grant Number 19K15000.

References

1. Y. Kitamura *et al.*, Jpn. J. Appl. Phys. 58 (2019) SGGD03.
2. Y. Iida *et al.*, Ultrason. Sonochem. **17** (2010) 480.
3. K. Yasui *et al.*, Phys. Rev. E **77** (2008) 016609.